Brain, Behavior, and Immunity 118 (2024) 355–363

Contents lists available at ScienceDirect

Brain Behavior and Immunity

journal homepage: www.elsevier.com/locate/ybrbi

Full-length Article

Targeting terminal pathway reduces brain complement activation, amyloid load and synapse loss, and improves cognition in a mouse model of dementia

Wioleta M. Zelek *, Ryan J. Bevan, Bryan Paul Morgan *

UK Dementia Research Institute Cardiff and Division of Infection and Immunity, School of Medicine, Cardiff University, Cardiff, Wales CF14 4XN, United Kingdom

ARTICLE INFO

Keywords:
Alzheimer's Disease
Complement
Membrane attack complex
Monoclonal antibody
Drugs

ABSTRACT

Complement is dysregulated in the brain in Alzheimer's Disease and in mouse models of Alzheimer's disease. Each of the complement derived effectors, opsonins, anaphylatoxins and membrane attack complex (MAC), have been implicated as drivers of disease but their relative contributions remain unclarified. Here we have focussed on the MAC, a lytic and pro-inflammatory effector, in the App^{NL-G-F} mouse amyloidopathy model. To test the role of MAC, we back-crossed to generate App^{NL-G-F} mice deficient in C7, an essential MAC component. C7 deficiency ablated MAC formation, reduced synapse loss and amyloid load and improved cognition compared to complement-sufficient App^{NL-G-F} mice at 8–10 months age. Adding back C7 caused increased MAC formation in brain and an acute loss of synapses in C7-deficient App^{NL-G-F} mice. To explore whether C7 was a viable therapeutic target, a C7-blocking monoclonal antibody was administered systemically for one month in App^{NL-G-F} mice aged 8–9 months. Treatment reduced brain MAC and amyloid deposition, increased synapse density and improved cognitive performance compared to isotype control-treated App^{NL-G-F} mice. The findings implicate MAC as a driver of pathology and highlight the potential for complement inhibition at the level of MAC as a therapy in Alzheimer's disease.

1. Introduction

The complement system is an important driver of inflammation in diverse settings, contributing to immune defence but, when dysregulated, causing tissue damage and pathology. In neurodegenerative diseases (NDDs), complement has been implicated both as a mediator of neuroinflammation and a direct cause of synapse loss (Hong et al., 2016; Carpanini et al., 2022; Bohlson & Tenner, 2023). Both the protective and pathological effects of complement are caused by the active products generated during complement activation; these comprise the small pro-inflammatory fragments C3a and C5a, the large opsonic fragments C3b, iC3b and C4b, and the cytotoxic membrane attack complex (MAC). The MAC, formed from the sequential assembly of the five terminal complement proteins C5b, C6, C7, C8 and C9, in the target cell membrane, creates a transmembrane pore that not only disrupts membrane integrity but also triggers inflammatory pathways in the target cell (Morgan, 2016; Zelek et al., (2019a)).We have previously shown that MAC is present and co-localises with pathology in the brain in Alzheimer's disease (AD), and that MAC contributes to synapse loss in the 3xTg mouse model of AD (Carpanini et al., 2022). Here we set out to further explore the contributions of complement dysregulation and MAC formation to pathology and cognition in an amyloid precursor protein (APP) knock-in mouse model of AD (Saito et al., 2014). These mice express human APP with the Swedish, Iberian and Arctic familial AD mutations in the *APP* gene ($APP^{NL/G/F}$); because of the way that they are engineered, artefacts caused by APP overexpression seen in transgenic models, including 3xTg, are avoided. The mice show an age-dependent accumulation of Aβ with amyloid plaques evident by 3 months, accompanied by synaptic loss, microgliosis and astrocytosis. Cognitive impairment is evident by 6 months. This early onset and rapid progression of disease makes these mice an excellent testbed for interventions. In order to test the contribution of MAC, we back-crossed the App^{NL-G-F} mice to C7 deficiency ($App^{NL-G-F}/C7^{-/-}$); absence of C7 eliminates the capacity to make the MAC pore but has no impact on upstream complement activation, including generation of C5a. Impact of C7 deficiency on pathology, complement dysregulation and cognition were tested and the effect on these parameters of adding back purified C7 explored. To ascertain whether C7 was a potential therapeutic target,

* Corresponding authors at: Cardiff University, Cardiff, Wales CF14 4XN, Wales, UK.
E-mail addresses: zelekw@cardiff.ac.uk (W.M. Zelek), morganbp@cardiff.ac.uk (B.P. Morgan).

https://doi.org/10.1016/j.bbi.2024.03.017
Received 5 December 2023; Received in revised form 28 February 2024; Accepted 11 March 2024
Available online 12 March 2024

App^{NL-G-F} mice were treated for 4 weeks with a mouse C7-blocking monoclonal antibody (mAb) previously shown to completely block systemic complement activity in wild-type mice (Zelek & Morgan, 2020). Impact on brain complement dysregulation, disease and cognition was assessed at end point in comparison with a control mAb.

2. Materials and methods

2.1. Reagents and sera

All chemicals, except where otherwise stated, were obtained from Fisher Scientific UK (Loughborough, UK) or Sigma Aldrich (Gillingham, UK) and were of analytical grade. All tissue culture reagents and plastics were from Invitrogen Life Technologies (Paisley, UK). Sheep erythrocytes in Alsever's solution were from TCS Biosciences (Claydon, UK). Human and animal sera were prepared in house from freshly collected blood. For human serum, blood was clotted at room temperature (RT) for 1 h (h), then placed on ice overnight for clot retraction before centrifugation and harvesting of serum. For mouse serum, blood was placed on ice 5 min after harvest and clotted for 2 h on ice before serum harvest. Sera were stored in aliquots at − 80 °C and not subjected to freeze–thaw cycles.

2.2. Animals

Mice were housed in groups in open-topped cages with 12-hour light/dark cycles and unlimited access to food and water. To produce homozygous C7-deficient mice, heterozygous C7 deficient mice (C57BL/6NJ-C7em1(IMPC)J/Mmjax C7+/-; Jackson ImmunoResearch, Baltimore, USA) were interbred in-house (Zelek & Morgan, 2020; Carpanini et al., 2022). App^{NL-G-F} knock-in mice expressing human APP with the Swedish (KM670/671NL), Iberian (I716F), and Arctic (E693G) mutations were generously provided by Dr. Takaomi Saido (Saito et al., 2014). Both males and females were used. Within each experiment, a single sex was used because the well-described differences in complement activity between male and female mice add a confounder to mixed-sex studies (Kotimaa et al., 2016). The UK Home Office Animals Scientific Procedures Act of 1986 and regional institutional policies were followed throughout every animal procedure. Mice were humanely sacrificed at the stated intervals using CO_2 asphyxia, then immediately perfused intracardially with phosphate buffered saline (PBS). Brains were removed, cut sagitally, one half fixed in 1.5 % (w/v) paraformaldehyde (PFA) for immunocytochemistry and DiOlistic spine labelling, and the other half snap frozen for ELISA experiments.

2.3. Testing the role of C7 in neurodegeneration in APP^{NL-G-F} mouse

To test whether C7, and by inference the MAC, contributed to neurodegeneration *in* App^{NL-G-F} mice, we first back-crossed onto C7 deficiency. Unmodified App^{NL-G-F} female mice were compared to co-housed C7-deficient (App^{NL-G-F} /$C7^{-/-}$) female mice at 8–9 months (7 mice per group). Single-gender groups were used in this and all other studies because of the known effects of gender on complement activity in mice (Kotimaa et al.,2016). Tests of cognition were performed as detailed below, brains harvested and complement activation, cytokine levels, amyloid load and synapse density measured as detailed in the sections below.

To confirm that the impact on the measured parameters was a direct effect of C7 deficiency, a C7 addback experiment was performed. App^{NL-G-F}/$C7^{-/-}$ mice (male, 8–10 months, 10 per group) were given either human C7 (in house affinity purified as described previously; Zelek & Morgan, 2020; Morgan, 2000) or PBS control, respectively, for a week. Human C7 was administered in three IP doses (16 mg/kg; 8 mg/kg; 8 mg/kg) at two-day intervals over a week. This dosing schedule was chosen from preliminary experiments that demonstrated near-physiological plasma C7 levels and complete block of haemolytic activity; the impact on complement activity was confirmed by measuring serum haemolytic activity prior to and during treatment using the CH50 assay described below.

To test whether systemically delivered anti-C7 blocking mAb influenced neurodegeneration, 8–9 month female App^{NL-G-F} mice were treated for one month with either the C7-blocking mAb 73D1 (n = 5) or D1.3 control IgG antibody (n = 5) delivered IP with an initial loading dose of 40 mg/kg followed by 20 mg/kg twice weekly. Impact on complement activity was confirmed by measuring haemolytic activity in blood samples taken prior to and during treatment using the CH50 assay described below.

2.4. CH50 haemolysis assay

Systemic complement activity in the mice was assessed using a classical pathway (CP) haemolysis assay (CH50) as previously described (Zelek & Morgan, 2020; Zelek et al., (2019b)). For assessment of C7 activity, a modified assay was developed (Zelek, 2021); the human and mouse terminal pathway components are highly compatible which allows use small amounts of mouse serum in the assay (Zelek & Morgan, 2020; Zelek, 2021). Antibody-sensitised sheep erythrocytes (ShEA; Amboceptor, Siemens, #ORLC25, Cruinn Diagnostics, Dublin, UK), at 2 % in HEPES-buffered saline containing Ca^{2+} and Mg^{2+} (HBS-Ca-Mg) were incubated with C7-depleted human serum (NHS-C7; 5 % in HBS-Ca-Mg) plus serial dilutions of normal mouse serum (NMS; 2.5 – 0 %) or the test mouse serum in duplicate in 96-well round-bottomed plates, incubated at 37 °C for 30 min, centrifuged and haemoglobin in the supernatant measured by absorbance at 405 nm. Percent haemolysis was calculated for each sample from the formula: % Lysis = Absorbance (Abs) sample - Abs background)/(Abs max - Abs background) x 100 %.

2.5. Preparation of mouse brain homogenates

Total brain homogenates (TBH) were prepared by homogenising the snap-frozen brain hemispheres for 5 min on ice in 0.3 ml of ice-cold Neuronal Protein Extraction Reagent (N-PER™; 87792, ThermoFisher Scientific, Loughborough, UK) containing 1x EDTA-free protease inhibitor (4693159001, Roche cOmplete mini EDTA-free, Sigma Aldrich). Homogenates were centrifuged at 13 000 rpm for 20 min at 4 °C, and supernatant (TBH) collected. The remaining pellet was further processed as previously described (Kaplan et al., 2003) to prepare the brain tissue bound protein (TBP) extracts that contain aggregated Aβ. In brief, pellets were resuspended in 0.3 ml 8 M Guanidine-HCl (24115, Thermofisher), homogenised on ice as described above, incubated on ice for 30 min, centrifuged as above, and the resulting supernatant (TBP) collected. Total protein concentration in TBH and TBP extracts was measured (Pierce Micro BCA Kit; 23235, Thermofisher) and concentrations adjusted by dilution to 40–70 mg/ml prior to aliquoting, snap freezing and storage at −80 °C until testing. Samples were not subjected to freeze–thaw cycles. Levels of all analytes measured in the ELISA described below were expressed relative to total protein measured using the BCA assay.

2.6. Detection of complement activation products in mouse brain homogenates

For detection of the terminal complex (TCC), a marker of terminal pathway activation and MAC formation, Maxisorp (ThermoFisher) 96-well plates were coated with rabbit anti-rat/mouse C9 (in-house; 10 μg/ml in bicarbonate buffer pH 9.6) and incubated at RT overnight (O/N). The wells were then blocked (30 min at 37 °C) with 3 % BSA in PBS 0.05 % Tween 20 (PBS-T) and rinsed in PBS-T. TBH were diluted to 0.5 mg/ml in PBS-T-EDTA (0.3 % BSA PBS with 10 mM EDTA), 50 μl aliquots added in duplicate to the ELISA wells and incubated O/N at 4 °C. Standard curves were generated using activated mouse serum, batch-generated by incubation with Zymosan A (7 mg/ml; Pierce, #21327)

and aggregated human IgG (50 μg/ml; in house) for 32 h at 37 °C in a shaking water bath, activating both classical and alternative pathways to completion. The reaction was stopped by centrifugation at 4600 rpm for 15 min at 4 °C and the supernatant (activated mouse serum; Act-NMS) collected and stored at − 80 °C in aliquots. For standard curves, Act-NMS) was double-diluted in PBS-T-EDTA from a starting dilution of 1:3 in duplicates. Wells were washed with PBS-T then incubated (1.5 hr, RT) with HRP-labelled detection antibody mAb 12C3 anti-mouse TCC-neoantigen mAb (in house; 5 μg/ml in PBS-T-EDTA). After washing plates were developed with OPD, and the absorbance (492 nm) was recorded.

To measure mouse C3b/iC3b/C3c, plates were coated with 2/11 mAb anti-mouse C3b/iC3b/C3c (5 μg/ml, HM1065, Hycult Biotech, Uden, Netherlands) and incubated O/N at RT. After blocking in 3 % BSA-PBS-T, plates were washed in PBS-T and TBH samples (1 in 800) were added, incubated O/N at 4 °C. The standard curve was generated using Act-NMS double-diluted in PBS-T-EDTA from a starting dilution of 1:1000 in duplicates. Plates were washed, and bound C3 fragments detected using in-house HRP-labelled rabbit anti-human C3 (cross-reactive with mouse C3), 1:500 in 0.3 % BSA-PBST-EDTA for 1.5 h at RT. Plates were washed twice, developed using OPD and absorbance quantified as above.

To determine the intra- and inter-assay precision (%CV; <10 %), two NMS samples (1 in 40 for TCC, and 1 in 20,000 for C3 fragments ELISA) were used as an inter-assay control across all plates and assays.

2.7. Detection of IL-1β by ELISA in mouse brain

IL-1β levels in TBH were measured using a commercial ELISA kit (DY401-05, R&D Systems) in accordance with the manufacturer's instructions. Briefly, wells were coated with capture antibody (1 in 250 in PBS, 100 μl/well) O/N at RT, washed, blocked, then incubated with 100 μl of TBH (1 in 2) or standards (serial dilutions: 0–1000 pg/ml). After washing, detection antibody was added and incubated, followed by streptavidin-HRP. Colour was developed using TMB, absorbance (450 nm) measured and IL-1β levels in the TBH samples read from the standard curve.

2.8. Detection of amyloid by ELISA in App^{NL-G-F} mouse brain

Human Aβ42 was measured in TBP extracts from App^{NL-G-F} mice (expressing human APP) using a commercial ELISA (Thermofisher, KHB3442) in accordance with the manufacturer's instructions. In short, TBP samples (1 in 8000) or standard (0–2000 pg/ml) were incubated in wells coated with capture antibody, wells washed, incubated with biotinylated detection antibody followed by streptavidin-HRP. Colour was developed with TMB, absorbance (450 nm) measured and Aβ42 levels in the TBP samples read from the standard curve.

2.9. DiOlistic spine labelling, imaging, and analyses

Fixed brains were cut into 60 μm thick sections using a Leica VT1200S vibratome; dorsal hippocampus regions from ten brain hemisphere sections per mouse were transferred to histology slides and neuronal DiOlistic labelling was performed as previously described (38–41). Briefly, 1,1′-Dioctadecyl-3,3,3′,3′-Tetramethylindocarbocyanine Perchlorate (DiI; Life Technologies)-coated 1 μm tungsten particles were fired into sections through an inverted cell culture insert (8.0 m; BD Falcon, BD Biosciences) at a pressure of 80–100 psi (Gene Gun system; BioRad). After incubation at RT for 1 h to permit dye diffusion, sections were fixed in 4 % PFA and mounted in FluorSave (Millipore).

Confocal images of sections were captured using the Leica SP8 Lightning confocal microscope (63x objective; z-axis interval 0.2 m) and the images deconvolved (Leica Lightning Deconvolution). Secondary apical dendrites from dye-labeled neurons in the CA1 hippocampal area were imaged to examine dendritic spine protrusions. To reduce operator bias, all images were blinded and processed as a single batch. Images were subjected to automated analysis using the Imaris FilamentTracer module (version 9.2, Bitplane, Zurich, Switzerland). The SpineClassifer MATLAB extension was used to classify the spine subtypes (stubby, mushroom, and thin) according to their morphologies.

2.10. Open-field and novel object recognition behavioural tests

All tests were performed with mice randomised and the operator blinded to group. Animals were acclimatised to the experimental room in their home cages for a week to minimize stress and the experiments were conducted in a dimly room with red lights.

The open-field (OF) test was carried out in a box (40 x 40 x 40 cm) with opaque sides. The mouse was placed in the middle of the box at the beginning of each trial, and its movements were video recorded for 7 min. The percentage of time spent in a marked central zone was captured by viewing the videos and measuring time spent in peripheral and central zones (Gellért & Varga, 2016).

Novel object recognition (NOR) testing was performed in the same 40 x 40 x 40 cm box but with visual cues included on the walls. Mice were first habituated to the box in the absence of objects on two consecutive days (10 min/ day). Next day (Day 1; training phase), two identical objects were presented for 10 min (A and A' objects) and time exploring each object measured. On Day 2 (test phase), the same mice were exposed for 10 min to an object familiar from the training (A) and a novel object (B) and time exploring each object recorded as before. Scent cues were eliminated from the box and objects by cleaning between trials (Huang & Hsueh, 2014).

2.11. Statistical analysis

GraphPad Prism Software (version 9.4.1, San Diego, California, USA) was used for statistical analyses. For *in vitro* investigations, bars denote the mean and standard error of the mean, and each data point represents a separate experiment that was carried out in duplicate. For in vivo experiments, all animals survived to the planned endpoint, and all data points were thus included in analysis. Each data point corresponds to one animal, and bars show means +/- SEM. The unpaired *t*-test was used to determine statistical significance between two groups, and one-way ANOVA was used for multiple groups. p-values of *p < 0.05, **p < 0.01, ***p < 0.001. All histopathologic quantification and analysis, including DiOlistics, were performed blinded to experimental groups. Each figure legend contains statistical information for each experiment and graph, including the statistical tests performed, the precise value of *n* (number of animals, samples), and dispersion and precision measurements (mean, SEM, etc.).

3. Results

3.1. C7 deficiency reduces brain complement dysregulation, amyloid load, synapse loss and cognitive impairment in App^{NL-G-F} mice

We have previously shown that App^{NL-G-F} mice have increased levels of complement activation products (C3b/iC3b/C3c and TCC) in brain homogenates compared to wild-type controls, demonstrating complement dysregulation in the brain (Carpanini et al., 2022). Here we explored the impact of C7 deficiency on complement dysregulation and its downstream effects in App^{NL-G-F} mice aged 8–9 months. Female $App^{NL-G-F}/C7^{-/-}$ mice had markedly reduced (to background) TCC levels in brain extracts (Fig. 1B; p = 0.0027) when compared to complement-sufficient female $App^{NL/G/F}$ mice; in contrast, levels of C3b/iC3b/C3c, an upstream activation product, were not impacted by C7 deficiency (Fig. 1B, p = 0.9042). $App^{NL-G-F}/C7^{-/-}$ mice showed significantly reduced levels of IL-1β (Fig. 1C; p = 0.0237) and Aβ in TBP (tissue bound protein) (Fig. 1D; p = 0.0482) in brain extracts compared to complement-sufficient matched App^{NL-G-F}. We chose to measure Aβ

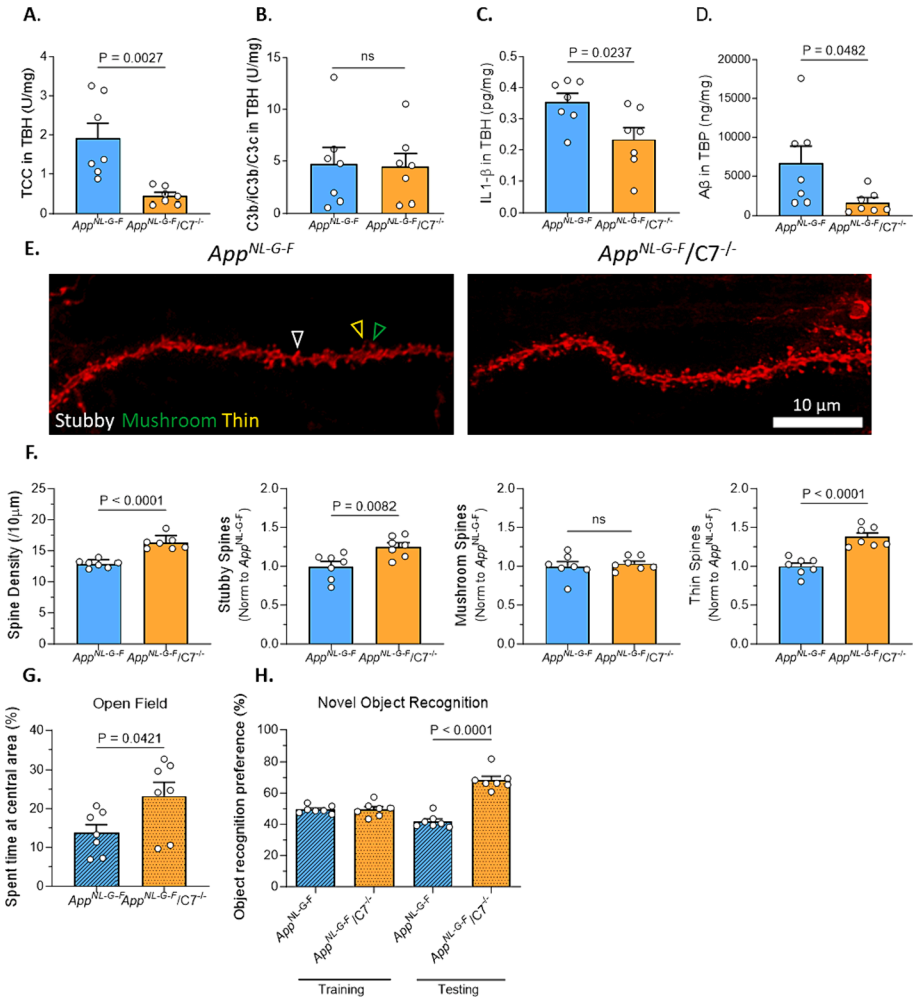

Fig. 1. C7 deficiency in female App^{NL-G-F} mice prevents MAC formation, decreases IL1-β and Aβ levels, protects synapses and improves cognition. A-D. Levels of complement activation products, IL1-β and Aβ peptides were measured in brain homogenates. A. Levels of C3 fragments (C3b/iC3b/C3c) measured in TBH (total brain homogenate) were not different between C7-deficient and complement-sufficient App^{NL-G-F} mice. B. Levels of the terminal complement complex (TCC) in TBH, high in App^{NL-G-F} mice, were reduced to background in C7-deficient App^{NL-G-F} mice. C. IL1-β levels in TBH, high in App^{NL-G-F} mice, were markedly reduced in C7-deficient App^{NL-G-F} mice. D. Levels of Aβ in TBP (tissue bound protein) were significantly decreased in C7-deficient App^{NL-G-F} mice. E,F. Assessment of hippocampal spine density in C7-deficient and sufficient App^{NL-G-F} female mice. E. Representative confocal images of DiOlistics labelled CA1 hippocampal dendritic segments (in red) in pre-fixed coronal brain slices. Spine densities were analysed from dendritic segments of at least 30 µm. Scale bar 5 µm. F. Spine density was significantly increased in App^{NL-G-F} /$C7^{-/-}$ compared to App^{NL-G-F} female mice ($p < 0.0001$); sub-analysis of different spine types showed that C7 deficiency significantly rescued stubby and thin spines. Data are normalised to App^{NL-G-F} levels (set at 1 in each) datapoints represent individual mice ($n = 7$ in each group). G, H. Comparison of C7-deficient and sufficient App^{NL-G-F} female mice in behavioural tests. G. In the open field (OF) test, C7-deficient mice spent significantly more time exploring the central area of the box ($p = 0.0421$). H. In the novel object recognition (NOR) tests, C7-deficient mice spent significantly more time exploring the novel object.

1–42 because of its pathological relevance and the robust elevation previously reported in App^{NL-G-F} mouse brain (Saito et al., 2014). Synapse number is reduced in App^{NL-G-F} mice compared to wildtypes and provides an early index of neurodegeneration in the model (Saito et al.,2014). To explore whether deficiency of C7 impacted synapse loss we measured synapse number using DiOlistics (Stafend & Meisel, 2011); brain sections from female App^{NL-G-F} and $App^{NL-G-F}/C7^{-/-}$ mice were imaged in identical areas in the CA1 region of the hippocampus; total spine number and numbers for the different morphological spine subtypes were automatically quantified using Imaris and ImageJ software as described in methods. Overall spine density was significantly higher in $App^{NL-G-F}/C7^{-/-}$ mice compared to App^{NL-G-F} controls (Fig. 1E,F; $p < 0.0001$). Comparison of the different morphological spine subtypes showed that this difference was greatest for thin and stubby spines (Fig. 1E, F; $p < 0.0001$, $p = 0.0082$ respectively).

Given that synapse density in the CA1 hippocampus region is associated with cognition and memory in mice and men (Morrison & Baxter, 2012, Perez-Cruz et al., 2011), we investigated whether the rescue of synapses observed in $App^{NL-G-F}/C7^{-/-}$ impacted memory. Performance of female App^{NL-G-F} and $App^{NL-G-F}/C7^{-/-}$ mice was compared in two behavioural tests, the open field (OF) and novel object recognition (NOR) tests. The OF test is a common measure of exploratory behaviour, while NOR tests object recognition memory. In the OF test, $App^{NL-G-F}/C7^{-/-}$ mice showed greater exploration, spending significantly more time in the centre of the test field compared to App^{NL-G-F} controls which moved less and favoured the field edges (Fig. 1G; $p = 0.0421$). In the NOR test the $App^{NL-G-F}/C7^{-/-}$ mice spent significantly more time exploring the novel object compared to App^{NL-G-F} (Fig. 1H, $p < 0.0001$).

3.2. C7 add-back in $App^{NL-G-F}/C7^{-/-}$ mice initiates MAC assembly, increases brain IL-1β and Aβ levels, exacerbates synapse loss and cognitive impairment

To confirm that the observed protective effect of C7 deficiency on

disease and cognition in the App^{NL-G-F} mice was caused by absence of MAC, male *App*$^{NL-G-F}$/C7$^{-/-}$ mice were given human C7 protein over a week in amounts that matched C7 levels in wildtype mice and fully restored serum haemolytic activity (Fig. 2A). Mice were subjected to behavioural testing on day 7 then sacrificed. Human C7 was detected in brain homogenates from all C7-treated *App*$^{NL-G-F}$/C7$^{-/-}$ mice but not in untreated *App*$^{NL-G-F}$/C7$^{-/-}$ mice (Fig. 2B). Levels of C3 fragments in brain homogenates were not impacted by administration of C7 (Fig. 2C; p = 0.7250); in contrast, levels of TCC, a readout for MAC formation, were significantly increased in C7-treated *App*$^{NL-G-F}$/C7$^{-/-}$ mice (Fig. 2D; p = 0.0130). Levels in brain homogenates of the inflammatory cytokine IL-1ß (Fig. 2E; p = 0.0492) and the APP-derived Aß peptide

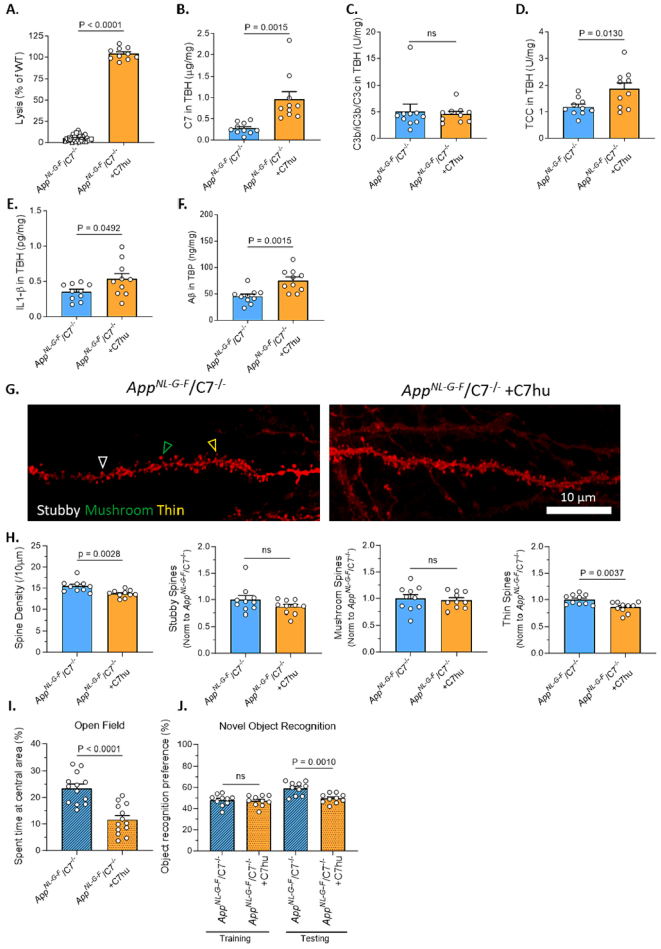

Fig. 2. C7 addback in C7-deficient *App*$^{NL-G-F}$ male mice causes brain complement dysregulation, MAC formation, increased IL1-β and Aβ levels, synapse loss and cognition deficit. A-F. C7-deficient *App*$^{NL-G-F}$ male mice administered human C7 for 7 days showed restored serum haemolytic activity (A) and human C7 was detectable in TBH (total brain homogenate) (B). While levels of C3 fragments in TBH was not impacted (C), TCC levels, indicative of MAC formation, were markedly increased after C7 administration (D). Levels of IL1-β in TBH (E) and Aβ in TBP (tissue bound protein) (F) were increased after 7 days of C7 addback. G, H. Representative confocal images of DiOlistics labelled CA1 hippocampal dendritic segments from C7-deficient *App*$^{NL-G-F}$ male mice after 7 days of administration of C7 or vehicle control (G). Scale bar 5 µm. Compared to controls, overall spine density was significantly reduced in the C7-treated group with thin spines most affected (H). I, J. Behavioural tests were conducted on C7-deficient *App*$^{NL-G-F}$ male mice after 7 days of administration of C7 or vehicle control. C7 addback caused significantly poorer performance in open field (OF; I) and novel object recognition (NOR; J) tests compared to vehicle controls. For all analyses, an unpaired two-tailed *t*-test was used to compare the two groups. Each point represents one animal. Error bars correspond to SEM and p values are included. ns = not significant.

(Fig. 2F, p = 0.0015) were significantly increased in *App*$^{NL-G-F}$/C7$^{-/-}$ mice following add-back of C7. Measurement of dendritic spines in CA1 hippocampus showed that administration of C7 for just one week in *App*$^{NL-G-F}$/C7$^{-/-}$ male mice caused a significant reduction in spine density compared to *App*$^{NL-G-F}$/C7$^{-/-}$ controls (Fig. 2G, H, p = 0.0028), with the thin spines being mainly impacted (Fig. 2H p = 0.0037). In the OF and NOR tests of cognition and memory, *App*$^{NL-G-F}$/C7$^{-/-}$ male given human C7 performed significantly less well compared to control *App*$^{NL-G-F}$/C7$^{-/-}$ male in both tests (Fig. 2I, J; p < 0.0001, p = 0.0010 respectively).

For all analyses, an unpaired two-tailed *t*-test was used to compare the two groups. Each point represents one animal. Error bars correspond to SEM and p values are included. ns = not significant.

3.3. *Systemic treatment with anti-C7 blocking mAb reduces MAC assembly, brain IL-1β and Aβ levels, synapse loss and cognitive impairment in App*$^{NL-G-F}$ *mice*

To investigate whether a tool anti-complement agent could inhibit complement dysregulation and MAC formation in the *App*$^{NL-G-F}$ mouse, we utilised our recently developed anti-C7 blocking mAb (73D.1; Zelek & Morgan, 2020). The mice were administered 73D1 anti-C7 mAb systemically over a month using a dosing schedule known to completely abrogate serum complement lytic activity in haemolysis assays. As expected, CP haemolytic activity in serum was suppressed in the 73D1-treated treated animals throughout the experiment whereas isotype control (D1.3) mAb had no effect (Fig. 3A, p < 0.0001). Mice were subjected to behavioural testing and then sacrificed on day 28. Levels of C3 fragments in brain homogenates were not impacted by administration of the anti-C7 mAb (Fig. 3B, p = 0.935); in contrast, levels of TCC, a readout for MAC formation, were more than halved in anti-C7-treated mice (Fig. 3C, p = 0.0152). Levels in brain homogenates of the inflammatory cytokine IL-1ß were reduced, albeit not significantly, in anti-C7-treated mice (Fig. 3D), while levels of Aß peptide were significantly reduced in TBP (tissue bound protein) (Fig. 3E, p = 0.0372). Measurement of dendritic spines in CA1 hippocampus showed that systemic administration of anti-C7 blocking mAb for a month in *App*$^{NL-G-F}$ female mice caused a significant increase in spine density compared to isotype control-treated *App*$^{NL-G-F}$ female controls (Fig. 3F), with rescue of thin spines predominating (Fig. 3G, p = 0.0156). In the OF and NOR tests, *App*$^{NL-G-F}$ female mice treated for 28 days with the anti-C7 mAb performed significantly better than isotype control-treated mice in both tasks (Fig. 3H, I, p < 0.0001, p = 0.0077 respectively).

4. Discussion

AD is the most prevalent type of dementia and is without an effective cure. The lack of a comprehensive understanding of the underlying pathological mechanisms is a significant obstacle to the development of AD therapies. Most current AD drugs, including the acetylcholine esterase inhibitors (galantamine, rivastigmine, tacrine, and donepezil) and N-methyl-D-aspartate receptor blockers (memantine), treat symptoms not the underlying pathology (Pardo-Moreno et al. (2022); Gupta et al.,2021; Imbimbo & Watling, 2021; Karran & De Strooper, 2022; Valiukas et al., 2022). The recent crop of anti-Aβ monoclonal antibodies entering the clinic (adunumab, lecanemab), while targeting and effectively clearing the hallmark amyloid plaque pathological markers, have a modest effect on disease progression and numerous toxicities (Haddad et al., 2022; Kuller & Lopez, 2021; Andrews et al., 2019; Salloway et al., 2022).

It is now clear that neuroinflammation is a significant factor in the development of neurodegeneration and an abundance of evidence that anti-inflammatory drugs might impact progression in AD (Lambert et al., 2013; Lambert et al., 2009; De Cordoba et al., 2012; Morgan et al., 2017; Cervellati et al., 2018; Franceschi et al. (2014); Tenner, 2020; Carpanini et al., 2019, Spangenberg & Green, 2017; Hoogland et al.,

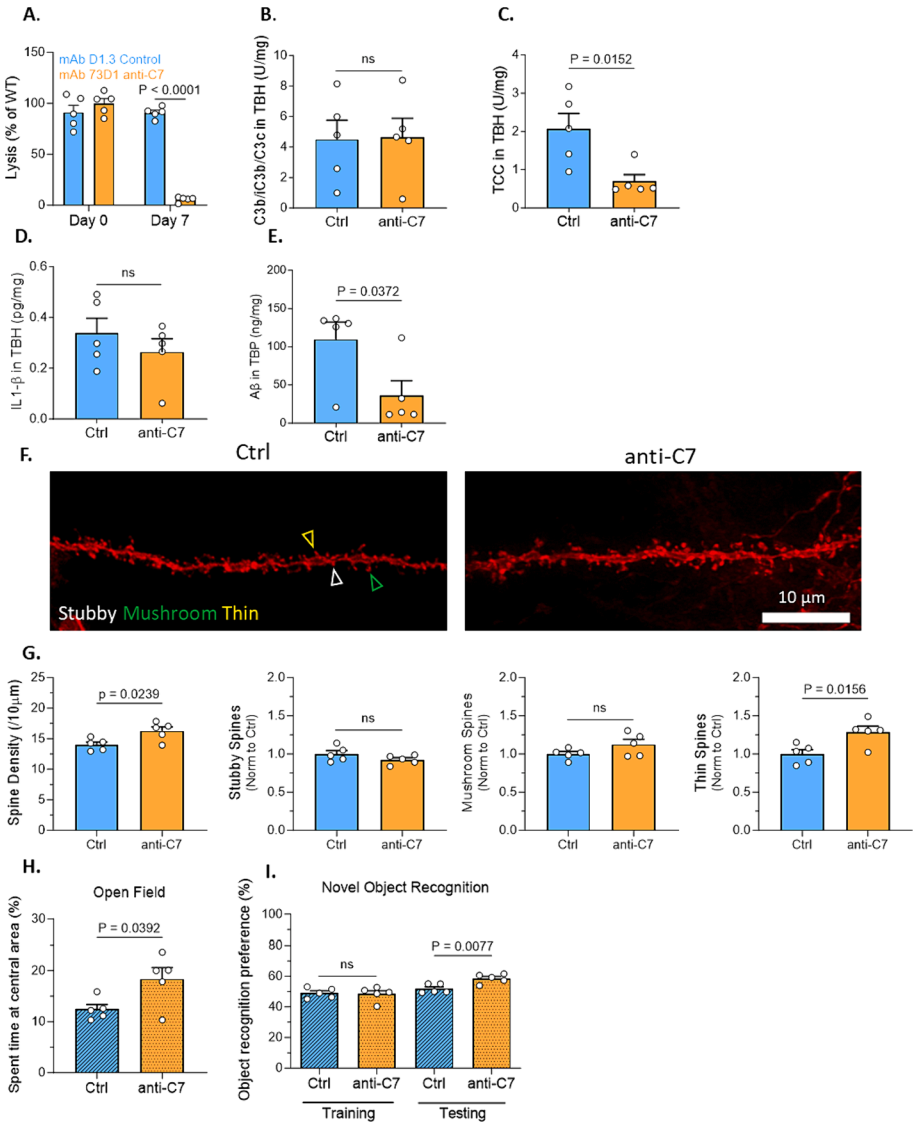

Fig. 3. Systemic administration of C7-blocking mAb inhibits brain complement activation, reduces IL1-β levels, Aβ levels and synapse loss, and improves cognition in female App^{NL-G-F} mice. A-E. Female App^{NL-G-F} mice aged 8–9 months were treated for a month with 73D1 anti-C7 mAb at a dose that completely blocked systemic complement or isotype control (A). While levels of C3 fragments in TBH were not impacted (B), TCC levels, indicative of MAC formation, were markedly reduced after anti-C7 administration when compared to isotype control (C). Levels of IL1-β in TBH (total brain homogenate) (D) and Aβ in TBP (tissue bound protein) (E) were significantly reduced after 28 days of anti-C7 treatment compared to controls. F, G. Representative confocal images of DiOlistics labelled CA1 hippocampal dendritic segments from App^{NL-G-F} female mice after 28 days of administration of anti-C7 or isotype control (F). Scale bar 5 µm. Compared to isotype control treated mice, overall spine density was significantly increased in the anti-C7-treated group with thin spines most affected (G). H, I. Behavioural tests were conducted on App^{NL-G-F} female mice after 28 days of administration of anti-C7 mAb or isotype control. Administration of anti-C7 significantly improved performance in open field (OF; H) and novel object recognition (NOR; I) tests compared to isotype controls. For all analyses, an unpaired two-tailed *t*-test was used to compare the two groups. Each point represents one animal. Error bars correspond to SEM and p values are included. ns = not significant.

2015; Zelek & Morgan, 2022; Schartz & Tenner, 2020). An understanding of the factors driving neuroinflammation in AD and other dementias would enable informed selection and better targeting of inflammation-blocking therapies. Complement, a potent driver of inflammation in many diseases, is strongly implicated in AD based on evidence from genetics, biomarkers and models (Lambert et al., 2013; Lambert et al., 2009; De Cordoba et al., 2012; Morgan et al., 2017; Veteleanu et al., 2023). Complement activation in the brain causes inflammation, activates and directs microglia and directly damages synapses, neurones and other brain cells (Bohlson & Tenner, 2023; Hong et al., 2016; Carpanini et al., 2022; Tenner, 2020; Daskoulidou et al., 2023; Schartz & Tenner, 2020). Of the several pro-inflammatory complement effectors, the MAC is uniquely relevant because it not only directly damages vulnerable targets but also activates diverse target cells to enhance inflammation (Morgan, 2016; Triantafilou et al., 2013; Zelek & Morgan, 2022; Carpanini et al., 2022). In brain, MAC damages synapses directly by "microlysis" and indirectly by triggering inflammatory pathways which in turn activate microglia.

We previously showed that C6 deficiency in the 3xTg AD model reduced synapse loss, implicating MAC in the process (Carpanini et al., 2022). This observation, together with the evidence that complement dysregulation in AD models involves activation of the terminal pathway with the generation of MAC, led us to investigate the pathological role of MAC in the App^{NL-G-F} AD mouse model and test the feasibility of targeting MAC for treatment of AD. We performed three experiments: first, we backcrossed App^{NL-G-F} mice to C7 deficiency ($App^{NL-G-F}/C7^{-/-}$); second, we added back human C7 to these $App^{NL-G-F}/C7^{-/-}$ mice; third, we treated the App^{NL-G-F} mice with a systemic anti-C7 mAb. In each

experiment, we examined the impact of the intervention on complement dysregulation in the brain, neuropathological parameters and cognitive state. For complement dysregulation we measured C3 activation products as an index of activation pathway dysregulation and TCC as an index of terminal pathway dysregulation and MAC formation. Brain levels of the APP-derived peptide Aβ were measured as an index of amyloid load, synapse density as a read-out for neurodegeneration and levels of the pro-inflammatory cytokine IL1-β as a marker of inflammasome-triggered inflammation, relevant to this study because we and others have shown that MAC is a potent activator of the inflammasome in diverse cell types (Morgan, 2016; Triantafilou et al., 2013). From the toolbox of behavioural tests in mice we selected Open Field (OF), a test of general locomotor ability and anxiety, and Novel Object Recognition (NOR), testing aspects of learning and memory (Gellért & Varga, 2016; Huang & Hsueh, 2014). These tests were selected for ease of use and to cover a broad range of behaviours. In preliminary studies we showed that C7 deficiency in wild-type mice at 2–3 months had no impact on synapse density.

Brain extracts from App^{NL-G-F} mice at 8 – 9 months contained substantial amounts of C3 fragments and TCC, demonstrating profound complement dysregulation involving the activation and terminal pathways. In the $App^{NL-G-F}/C7^{-/-}$ mice, C3 fragment levels in brain extracts were elevated to the same degree as App^{NL-G-F}; in contrast, TCC levels were at assay background, demonstrating that absence of C7 had blocked terminal pathway activation and MAC formation. Absence of MAC was associated with decreased amyloid load in brain as assessed by measuring the APP-derived peptide Aβ, and with reduced levels of the inflammatory cytokine IL-1ß, reflecting elimination of MAC-triggered inflammasome activation in brain cells (Triantafilou et al., 2013). Although we do not address the source of IL-1ß in this study, microglia are known to express inflammasome components and are the primary source of IL-1ß in the inflamed brain (Yao et al., 2023). Remarkably, $App^{NL-G-F}/C7^{-/-}$ mice had significantly reduced levels of Aß peptides in brain extracts, indicating a decreased amyloid load compared to App^{NL-G-F} controls. We are currently investigating whether the reduction in neuroinflammation associated with absence of MAC is responsible for reduced amyloid load. Compared to App^{NL-G-F} controls, $App^{NL-G-F}/C7^{-/-}$ mice had significantly greater numbers of synaptic spines measured in CA1 hippocampus; indeed, numbers were similar to those measured in wildtype mice of the same age (Bevan et al., 2020). These data are congruent with our previous demonstration that C6 deficiency caused reduced synapse loss in 3xTg mice and further support our suggestion that MAC directly damages synapses (Bevan et al., 2020; Carpanini et al., 2022). Hippocampal synapse loss is strongly associated with cognitive impairment in man and models (Morrison & Baxter, 2012, Perez-Cruz et al., 2011; Frankfurt and Luine, 2015; Subramanian et al., 2020), and App^{NL-G-F} mice have age-dependent cognitive deficits from ~ 6 months of age (Whyte et al., 2017; Mehla et al. (2018)). We showed that $App^{NL-G-F}/C7^{-/-}$ mice tested at 8–9 months performed significantly better than matched App^{NL-G-F} controls in open field and novel object recognition tests, confirming a rescue of cognitive function.

To further confirm the role of MAC, we then administered human C7 to the $App^{NL-G-F}/C7^{-/-}$ mice for a week to restore capacity to generate MAC. Human and mouse terminal pathway proteins are compatible between species, as confirmed here by the restoration of serum haemolytic activity. The add-back of human C7 was restricted to just one week because the immune response to the human protein generates neutralising antibodies beyond this time (Mead et al., 2002). Functional restoration was confirmed systemically by demonstrating full haemolytic activity in serum and centrally by showing a marked increase (from baseline) of TCC levels in brain and human C7 protein detected in brain. Entry of C7 (Mr ~ 105 kDa) into the brain confirms previous reports of blood brain barrier (BBB) impairment in the App^{NL-G-F} mouse (Xie et al. (2021)). Restoration of capacity to generate MAC for just one week acutely increased IL1-ß and Aß peptide levels in brain homogenates, caused a significant decrease of neuronal synaptic density and reduced performance in the OF and NOR cognitive tests compared to vehicle-treated $App^{NL-G-F}/C7^{-/-}$ mice. The effects of C7 restoration for just one week are remarkable, demonstrating an acute effect of MAC, likely by inducing acute inflammation via NLRP3 activation and direct destruction of synapses. In support of this, others have shown that inflammation, and specifically IL-1β, can trigger degeneration of neurons and formation of Aβ aggregates (Bai and Zhang (2021)). The rapid impact of restoring MAC reflects the fact that early stages of complement dysregulation continue in the $App^{NL-G-F}/C7^{-/-}$ brain, priming for rapid terminal pathway activation on restoring C7. These findings also imply that absence of MAC and associated inflammation, rather than reduced accumulation of Aß, are responsible for the impact on neurodegeneration and behaviour.

Given that the absence of MAC is protective, and its presence exacerbates AD pathology in the App^{NL-G-F} mouse, we investigated the therapeutic possibility of systemic blockage of MAC formation in vivo. We have previously reported that two weeks systemic treatment of 6 month old App^{NL-G-F} mice with the anti-C7 mAb 73D1 had no effect on overall synapse number in CA1 hippocampus; however, we did find a significant increase in synapses in *peri*-plaque regions (Carpanini et al., 2022). Others have shown that therapeutic anti-amyloid mAb delivered systemically in App^{NL-G-F} mice at either 3–5 months or 7–9 months accesses the brain, albeit markedly better in the older mice (Gustavsson et al., 2023). These findings provoked us to repeat the study in older App^{NL-G-F} mice (9 months) in which the BBB is likely more impaired (Xie et al. (2021)), treated systemically for four weeks with the anti-C7 mAb. Compared to isotype control-treated App^{NL-G-F}, systemic administration of mAb 73D1 for 4 weeks at a dose that completely blocked systemic complement lytic activity, caused a significant reduction in levels of TCC in brain homogenates, confirming target engagement. Brain IL1-ß levels were markedly reduced in anti-C7-treated App^{NL-G-F} mice, as were Aβ levels in brain protein extracts. Anti-C7 treatment significantly increased overall hippocampal synaptic spine density and improved performance in the OF and NOR cognitive tests compared to isotype control treated App^{NL-G-F} mice, demonstrating a marked impact of the anti-C7 mAb on biomarkers, pathology and behaviour. There is an abundance of literature linking spine density to behaviour and cognition in different AD (and other NDD) models in rodents (Frankfurt & Luine, 2015; Subramanian et al., 2020). Neuronal network features can be affected by subtle changes in dendritic spine densities or size, which may result in altered moods or cognitive functions, problems with learning and memory, and hypersensitivity to pain. (Gipson & Olive, 2017). In our experiments the spines that were predominantly affected were thin spines, thought to be particularly plastic and linked to learning. Also demonstrated by the cognitive improvements that are related to the higher number of thin spines.

5. Conclusions

Others have reported that C3 deficiency in the APP/PS1 mouse AD model was associated with significantly better performance on learning and memory tasks (Shi et al., 2017); here we confirm that complement deficiency preserves cognition in an AD model and identify the MAC as a critical factor. Our data show that complement dysregulation and MAC formation are important drivers of pathology in the App^{NL-G-F} mouse AD model and suggest that MAC is a valid therapeutic target for AD. They confirm that the BBB is sufficiently impaired in 9 month old App^{NL-G-F} mice to allow entry of systemically administered anti-C7 mAb into the brain, enough to block all available C7, stop MAC formation, reduce brain inflammation and amyloid deposition, reduce synapse loss and improve cognition. Because this approach relies on BBB impairment associated with advanced pathology, it is likely that treatment with unmodified anti-C7 mAb earlier in the disease process would be ineffective because the mAb would be excluded. To counter this and enable treatment of early disease, much more relevant to human AD, our current focus is on development of BBB-penetrant C7-blocking mAb or

other moieties.

Author contributions

RJB and WMZ performed the laboratory analysis. BPM and WMZ designed the experiments. WMZ wrote the first draft of the manuscript. All authors read and approved the final version of the manuscript.

CRediT authorship contribution statement

Wioleta M. Zelek: . **Ryan J. Bevan:** Visualization, Methodology, Formal analysis, Data curation. **Bryan Paul Morgan:** Writing – review & editing, Visualization, Validation, Supervision, Resources, Project administration, Methodology, Investigation, Funding acquisition, Formal analysis, Data curation, Conceptualization.

Declaration of Competing Interest

The authors declare that they have no known competing financial interests or personal relationships that could have appeared to influence the work reported in this paper.

Data availability

Data will be made available on request.

Acknowledgments

This work is supported by the UK Dementia Research Institute which receives its funding from UK DRI Ltd, funded by the UK Medical Research Council, Alzheimer's Society and Alzheimer's Research UK. WMZ is supported by Race Against Dementia Alzheimer's Research UK Fellowship Award.

References

Andrews, J.S., Desai, U., Kirson, N.Y., Zichlin, M.L., Ball, D.E., Matthews, B.R., 2019. Disease severity and minimal clinically important differences in clinical outcome assessments for alzheimer's disease clinical trials. Alzheimers Dement (n y). 5, 354–363. https://doi.org/10.1016/j.trci.2019.06.005.

Bai, H., Zhang, Q., 2021. Activation of NLRP3 inflammasome and onset of alzheimer's disease. Front Immunol. 12, 701282 https://doi.org/10.3389/fimmu.2021.701282.

Bevan, R.J., Hughes, T.R., Williams, P.A., Good, M.A., Morgan, B.P., Morgan, J.E., 2020. Retinal ganglion cell degeneration correlates with hippocampal spine loss in experimental alzheimer's disease. Acta Neuropathol Commun. 8 (1), 216. https://doi.org/10.1186/s40478-020-01094-2.

Bohlson, S.S., Tenner, A.J., 2023. Complement in the brain: contributions to neuroprotection, neuronal plasticity, and neuroinflammation. Annu Rev Immunol. 26 (41), 431–452. https://doi.org/10.1146/annurev-immunol-101921-035639.

Carpanini, S.M., Torvell, M., Morgan, B.P., 2019. Therapeutic inhibition of the complement system in diseases of the central nervous system. Front Immunol. 10, 362. https://doi.org/10.3389/fimmu.2019.00362.

Carpanini, S.M., Torvell, M., Bevan, R.J., Byrne, R.A.J., Daskoulidou, N., Saito, T., Morgan, B.P., 2022. Terminal complement pathway activation drives synaptic loss in alzheimer's disease models. Acta Neuropathol Commun. 10(1):99.

Cervellati, C., Trentini, A., Bosi, C., Valacchi, G., Morieri, M.L., Zurlo, A., Brombo, G., Zuliani, G., 2018. Low-grade systemic inflammation is associated with functional disability in elderly people affected by dementia. Geroscience. 40 (1), 61–69. https://doi.org/10.1007/s11357-018-0010-6.

Daskoulidou, N., Shaw, B., Torvell, M., Watkins, L., Cope, E.L., Carpanini, S.M., Morgan, B.P., 2023. Complement receptor 1 is expressed on brain cells and in the human brain. Glia. 71 (6), 1522–1535. https://doi.org/10.1002/glia.24355.

de Cordoba, S.R., Tortajada, A., Harris, C.L., Morgan, B.P., 2012. Complement dysregulation and disease: from genes and proteins to diagnostics and drugs. Immunobiology. 217 (11), 1034–1046. https://doi.org/10.1016/j.imbio.2012.07.021.

Franceschi, C., Campisi, J. Chronic inflammation (inflammaging) and its potential contribution to age-associated diseases. 2014. J. Gerontol. A Biol. Sci. Med. Sci. 69: S4–S9. https://doi.org/10.1093/gerona/glu057.

Frankfurt, M., Luine, V., 2015. The evolving role of dendritic spines and memory: interaction(s) with estradiol. Horm Behav. 74, 28–36. https://doi.org/10.1016/j.yhbeh.2015.05.004.

Gellért, L., Varga, D., 2016. Locomotion activity measurement in an open field for mice. Bio-Protocol. 6 (13) https://doi.org/10.21769/BioProtoc.1857.

Gipson, C.D., Olive, M.F., 2017. Structural and functional plasticity of dendritic spines - root or result of behavior? Genes Brain Behav. 16 (1), 101–117. https://doi.org/10.1111/gbb.12324.

Gupta, G.L., Samant, N.P., 2021. Current druggable targets for therapeutic control of alzheimer's disease. Contemp Clin Trials. 109, 106549 https://doi.org/10.1016/j.cct.2021.106549.

Gustavsson, T., Metzendorf, N.G., Wik, E., Roshanbin, S., Julku, U., Chourlia, A., Sehlin, D., 2023. Long-term effects of immunotherapy with a brain penetrating aβ antibody in a mouse model of alzheimer's disease. Alzheimers Res Ther. 15 (1), 90. https://doi.org/10.1186/s13195-023-01236-3.

Haddad, H.W., Malone, G.W., Comardelle, N.J., Degueure, A.E., Kaye, A.M., Kaye, A., D., 2022. Aducanumab, a novel anti-amyloid monoclonal antibody, for the treatment of alzheimer's disease: a comprehensive review. Health Psychol Res. 10 (1), 31925. https://api.semanticscholar.org/CorpusID:246438511.

Hong, S., Beja-Glasser, V.F., Nfonoyim, B.M., Frouin, A., Li, S., Ramakrishnan, S., Stevens., B. 2016. Complement and microglia mediate early synapse loss in Alzheimer mouse models. Science. 6;352(6286):712-716. https://www.science.org/doi/10.1126/science.aad8373.

Hoogland, I.C., Houbolt, C., van Westerloo, D.J., van Gool, W.A., van de Beek, D., 2015. Systemic inflammation and microglial activation: systematic review of animal experiments. J Neuroinflammation. 12, 114. https://doi.org/10.1186/s12974-015-0332-6.

Huang, T.N., Hsueh, Y.P., 2014. Novel object recognition for studying memory in mice. Bio-Protocol. 4, e1249. https://doi.org/10.21769/BioProtoc.1249.

Imbimbo, B.P., Watling, M., 2021. What have we learned from past failures of investigational drugs for alzheimer's disease? Expert Opin Investig Drugs. 30 (12), 1175–1182. https://doi.org/10.1080/13543784.2021.2017881.

Karran, E., De Strooper, B., 2022. The amyloid hypothesis in alzheimer disease: new insights from new therapeutics. Nat Rev Drug Discov. 21 (4), 306–318.

Kotimaa, J., Klar-Mohammad, N., Gueler, F., Schilders, G., Jansen, A., Rutjes, H., van Kooten, C., 2016. Sex matters: systemic complement activity of female C57BL/6J and BALB/CJ mice is limited by serum terminal pathway components. Mol Immunol. 76, 13–21. https://doi.org/10.1016/j.molimm.2016.06.004.

Kuller, L.H., Lopez, O.L., 2021. ENGAGE and EMERGE: truth and consequences? Alzheimers Dement. 17 (4), 692–695. https://doi.org/10.1002/alz.12286.

Lambert, J.C., Heath, S., Even, G., Campion, D., Sleegers, K., Hiltunen, M., Amouyel, P., 2009. Genome-wide association study identifies variants at CLU and CR1 associated with alzheimer's disease. Nat Genet. 41 (10), 1094–1099. https://www.nature.com/articles/ng.439.

Lambert, J.C., Ibrahim-Verbaas, C.A., Harold, D., Naj, A.C., Sims, R., Bellenguez, C., Amouyel, P., 2013. Meta-analysis of 74,046 individuals identifies 11 new susceptibility loci for alzheimer's disease. Nat Genet. 45 (12), 1452–1458.

Mead, R.J., Singhrao, S.K., Neal, J.W., Lassmann, H., Morgan, B.P., 2002. The membrane attack complex of complement causes severe demyelination associated with acute axonal injury. J Immunol. 168 (1), 458–465. https://doi.org/10.4049/jimmunol.168.1.458.

Mehla, J., Lacoursiere, S.G., Lapointe, V., McNaughton, B.L., Sutherland, R.J., McDonald, R.J., Mohajerani, M.H., 2019. Age-dependent behavioral and biochemical characterization of single APP knock-in mouse (APPNL-G-F/NL-G-F) model of alzheimer's disease. Neurobiol Aging. 75, 25–37. https://doi.org/10.1016/j.neurobiolaging.2018.10.026.

Morgan, B.P., 2000. Complement methods and protocols. Humana Press.

Morgan, B.P., 2016. The membrane attack complex as an inflammatory trigger. Immunobiology. 221 (6), 747–751. https://doi.org/10.1016/j.imbio.2015.04.006.

Morgan, A.R., Touchard, S., O'Hagan, C., Sims, R., Majounie, E., Escott-Price, V., Morgan, B.P., 2017. The correlation between inflammatory biomarkers and polygenic risk score in alzheimer's disease. J Alzheimers Dis. 56 (1), 25–36. https://doi.org/10.3233/JAD-160889.

Morrison, J.H., Baxter, M.G., 2012. The ageing cortical synapse: hallmarks and implications for cognitive decline. Nat Rev Neurosci. 13 (4), 240–250.

Pardo-Moreno, T., González-Acedo, A., Rivas-Domínguez, A., García-Morales, V., García-Cozar, F.J., Ramos-Rodríguez, J.J., Melguizo-Rodríguez, L., 2022. Therapeutic approach to alzheimer's disease: current treatments and new perspectives. Pharmaceutics. 14 (6), 1117. https://doi.org/10.3390/pharmaceutics14061117.

Perez-Cruz, C., Nolte, M.W., van Gaalen, M.M., Rustay, N.R., Termont, A., Tanghe, A., Ebert, U., 2011. Reduced spine density in specific regions of CA1 pyramidal neurons in two transgenic mouse models of alzheimer's disease. J Neurosci. 9;31(10): 3926–34 https://doi.org/10.1523/JNEUROSCI.6142-10.2011.

Saito, T., Matsuba, Y., Mihira, N., Takano, J., Nilsson, P., Itohara, S., Saido, T.C., 2014. Single app knock-in mouse models of alzheimer's disease. Nat Neurosci. 17 (5), 661–663.

Salloway, S., Chalkias, S., Barkhof, F., Burkett, P., Barakos, J., Purcell, D., Smirnakis, K., 2022. Amyloid-related imaging abnormalities in 2 phase 3 studies evaluating aducanumab in patients with early alzheimer disease. JAMA Neurol. 79 (1), 13–21. https://doi.org/10.1001/jamaneurol.2021.4161.

Schartz, N., Tenner, A., 2020. The good, the bad, and the opportunities of the complement system in neurodegenerative disease. J. Neuroinflammation. 17 (1), 354. https://doi.org/10.1186/s12974-020-02024-8.

Shi, Q., Chowdhury, S., Ma, R., Le, K.X., Hong, S., Caldarone, B.J., Lemere, C.A., 2017. Complement C3 deficiency protects against neurodegeneration in aged plaque-rich APP/PS1 mice. Sci Transl Med. 9(392):eaaf6295. https://www.science.org/doi/10.1126/scitranslmed.aaf6295.

Spangenberg, E., Green, K.N., 2017. Inflammation in alzheimer's disease: lessons learned from microglia-depletion models. Brain Behav. Immun. 61, 1–11. https://doi.org/10.1016/j.bbi.2016.07.003.

Stafend, N.A., Meisel, R.L., 2011. DiOlistic labeling in fxed brain slices: phenotype, morphology, and dendritic spines. Curr Protoc Neurosci. 2 (2), 13. https://doi.org/10.1002/0471142301.ns0213s55.

Subramanian, J., Savage, J.C., Tremblay, M.È., 2020. Synaptic loss in alzheimer's disease: mechanistic insights provided by two-photon in vivo imaging of transgenic mouse models. Front Cell Neurosci. 14, 592607 https://doi.org/10.3389/fncel.2020.592607.

Tenner, A., 2020. Complement-mediated events in alzheimer's disease: mechanisms and potential therapeutic targets. J. Immunol. 204, 306–315. https://doi.org/10.4049/jimmunol.1901068.

Triantafilou, K., Hughes, T.R., Triantafilou, M., Morgan, B.P., 2013. The complement membrane attack complex triggers intracellular Ca2+ fluxes leading to NLRP3 inflammasome activation. J Cell Sci. 126 (Pt 13), 2903–2913. https://doi.org/10.1242/jcs.124388.

Valiukas, Z., Ephraim, R., Tangalakis, K., Davidson, M., Apostolopoulos, V., Feehan, J., 2022. Immunotherapies for alzheimer's D, isease-a review. Vaccines. 10 (9), 1527. https://doi.org/10.3390/vaccines10091527.

Veteleanu, A., Stevenson-Hoare, J., Keat, S., Daskoulidou, N., Zetterberg, H., Heslegrave, A., Morgan, B.P., 2023. Alzheimer's disease-associated complement gene variants influence plasma complement protein levels. J Neuroinflammation. 20 (1), 169. https://doi.org/10.1186/s12974-023-02850-6.

Whyte, L.S., Hemsley, K.M., Lau, A.A., Hassiotis, S., Saito, T., Saido, T.C., Sargeant, T.J., 2017. Reduction in open field activity in the absence of memory deficits in the AppNL-G-F knock-in mouse model of alzheimer's disease. Behav Brain Res. 336, 177–181. https://doi.org/10.1016/j.bbr.2017.09.006.

Xie, J., Gorle, N., Vandendriessche, C., Van Imschoot, G., Van Wonterghem, E., Van Cauwenberghe, C., Van Hoecke, L., Vandenbroucke, R.E., 2021. Low-grade peripheral infammation afects brain pathology in the APP(NL-G-F) mouse model of alzheimer's disease. Acta Neuropathol Commun. 9, 163. https://doi.org/10.1186/s40478-021-01253-z.

Yao, J., Wang, Z., Song, W., Zhang, Y., 2023. Targeting NLRP3 inflammasome for neurodegenerative disorders. Mol Psychiatry. https://doi.org/10.1038/s41380-023-02239-0.

Zelek, W.M., 2021. Measuring Total classical pathway and activities of individual components of the mouse complement pathway. Bio Protoc. 11 (19), e4175. https://doi.org/10.21769/BioProtoc.4175.

Zelek, W.M., Morgan, B.P., 2020. Monoclonal antibodies capable of inhibiting complement downstream of C5 in multiple species. Front Immunol. 10 (11), 612402 https://doi.org/10.3389/fimmu.2020.612402.

Zelek, W.M., Morgan, B.P., 2022. Targeting complement in neurodegeneration: challenges, risks, and strategies. Trends Pharmacol Sci. 43 (8), 615–628. https://doi.org/10.1016/j.tips.2022.02.006.

Zelek, W.M., Taylor, P.R., Morgan, B.P., 2019a. Development and characterization of novel anti-C5 monoclonal antibodies capable of inhibiting complement in multiple species. Immunology. 157 (4), 283–295. https://onlinelibrary.wiley.com/doi/10.1111/imm.13083.

Zelek, W.M., Xie, L., Morgan, B.P., Harris, C.L., 2019b. Compendium of current complement therapeutics. Mol Immunol. 114, 341–352. https://doi.org/10.1016/j.molimm.2019.07.030.